ORBIT-SPIN COUPLING AND MARTIAN EARLY-SEASON GLOBAL-SCALE DUST STORMS: CHALLENGES AND OPPORTUNITIES

J. H. Shirley , *TORQUEFX, Simi Valley, CA, USA,* **J. M. Battalio**, *Department of Geology and Geophysics, Yale University, New Haven, CT, USA,* **D. M. Kass**, *Jet Propulsion Laboratory, Pasadena CA, USA,* **A. Kleinböhl**, *Jet Propulsion Laboratory, Pasadena CA, USA,* **N. G. Heavens**, *Space Science Institute, Boulder, CO, USA,* **S. Piqueux**, *Jet Propulsion Laboratory, Pasadena CA, USA,* **S. Suzuki**, *Jet Propulsion Laboratory, Pasadena CA, USA,* **D, J. McCleese**, *Synoptic Sciences, Pasadena, CA, USA,* **J. T. Schofield**, *Jet Propulsion Laboratory (retired), Pasadena CA, USA.*

Introduction: The seven known Martian early-season global dust storms (GDS) of the historic record have at least two things in common: In addition to their early inception dates (L_s<235°), all seven occurred during intervals when Martian orbit-spin coupling torques were rapidly changing (Fig. 1).

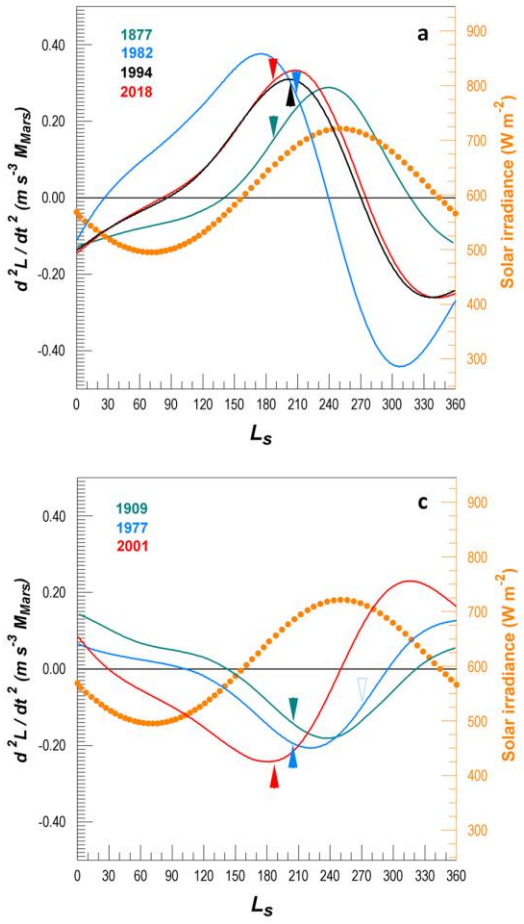

Fig. 1. The second time derivative of Mars' orbital angular momentum, a proxy for the rate of change of orbit-spin coupling torques, for Mars years with early-season GDS (1877, 1909, 1977, 1982, 1994, 2001, 2018). After Fig. 8 of Shirley et al. (2020). Dotted symbols indicate solar irradiance.

Numerical modeling investigations have had limited success in simulating early-season GDS. One notable success is found in the study by Newman et al. (2019), where a GDS was correctly simulated in the 1982 model year, with a modeled inception date of L_s=201° (versus an observed date of L_s=208°). Orbit-spin coupling accelerations (Shirley, 2017) were included within the dynamical core of the MarsWRF MGCM for that study. Century-long model runs performed in this configuration replicated the historic record of Mars years with and without GDS with a hindcast success rate of nearly 80% (Shirley, Newman et al., 2019). The temporal alignment between MGCM simulations and historic GDS observations is significantly improved by the addition of orbit-spin coupling accelerations (Mischna & Shirley, 2017; Shirley, Newman et al., 2019).

Orbit-spin coupling: A novel form of coupling between the orbital and rotational motions of extended bodies is given by:

$$CTA = - c\,(\dot{\boldsymbol{L}} \times \boldsymbol{\omega}_a) \times \mathbf{r}$$

Here *CTA* stands for "coupling term acceleration", $\boldsymbol{L}$ is the orbital angular momentum of a solar system extended body with respect to an inertial frame, $\boldsymbol{\omega}_a$ is the angular velocity of the planetary rotation, and **r** is a position vector identifying some specific location on or within the extended body. The leading term (-*c*) is a coupling efficiency coefficient, which is analogous to the coefficient of friction employed in mechanical problems. The specified acceleration field takes the form of a reversing torque, with complex time variability, and with axis lying in the equatorial plane of the affected body (Fig. 2).

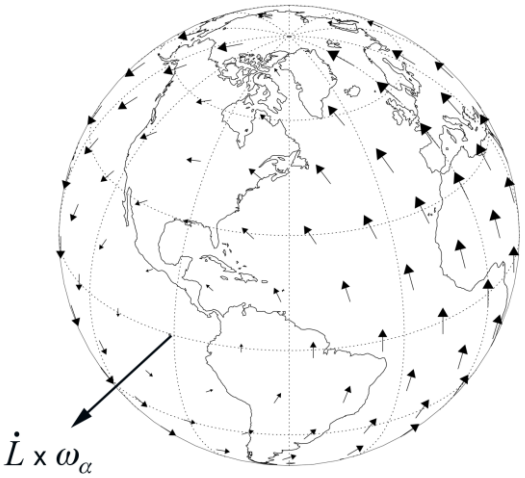

Fig. 2. *CTA* (surface) acceleration vectors, comprising a torque (here, on the Earth) about the axis indicated (see http://arxiv.org/abs/2112.02186).

The reader may visualize the planet rotating beneath, or within, the acceleration field of Fig. 2. When the forcing function ($\dot{\boldsymbol{L}}$) changes sign, the surface vectors of Fig. 2 will shrink and disappear, thereafter re-emerging with reversed directions. While the coupling efficiency parameter *c* may appear arbitrary, the results of the investigations performed to date indicate that nature does indeed prefer and employ a non-zero value of *c* in this connection. *c* helps to quantify the fraction of the orbital momentum that may participate in the excitation of dissipative geophysical variability (Shirley, 2017).

Somewhat misleadingly, in Mischna & Shirley (2017), the accelerations were characterized as a small effect, since the coupling is, from a planetary dynamical perspective, a weak one. Simulations performed in the same study revealed a modulation of Martian global wind speeds by factors of up to ~20%. This cannot accurately be described as a small effect!

The prior numerical modeling efforts by Mischna & Shirley (2017) and Newman et al. (2019) were barely able to scratch the surface, as these were hampered by limited funding and other issues. Important metrics, such as the time variability of atmospheric momentum and energy, were neglected. The spatial grid sizes employed were (at 5° x 5°) too coarse to allow investigation of smaller scale phenomena. Thus, multiple opportunities now exist to rapidly advance our understanding through new modeling. Here we highlight two insights gained *after* the prior modeling studies were completed, and pose a new question pertaining to the triggering processes of early-season GDS (Fig. 1).

Frictional damping of an intensified meridional overturning circulation (MOC): Intermittent intensification of Hadley-type meridional circulation cells was recognized as a key consequence of *CTA* forcing of the large-scale circulation in Mischna & Shirley (2017). The intensification may be characterized as a "diagnostic observable."

We ask: What is the time required to go from the spun-up, or loaded, atmospheric state, to an unloaded, unforced condition, under the assumption of a rapid disappearance of the driving accelerations?

Calculations addressing the relaxation time of an intensified Hadley-type circulation are presented in Shirley et al. (2020). Figure 3 illustrates the source data (a) and the system diagram (b) for the calculation. Figure 3a illustrates the *difference* between a forced simulation and a control simulation; here the brown colors represent the intensification of a zonally averaged clockwise MOC, as simulated by MarsWRF, averaged over an interval of 20° of L_s, prior to the inception of the 1982 GDS. The cartoon of Fig. 3b represents the same mean zonal circulation. We modeled the retardation of this circulation by surface friction forces as a function of time. Space limitations prevent a complete description of the model; however, the following high-level attributes are of interest. The linear velocity of the forced circulation near the surface exceeds than that of the control simulation by ~3.6 m s^{-1}, and the sequestered energy associated with the intensified MOC is ~7 x 10^{17} J. Employing diurnally averaged values for surface wind stresses of 0.001 Nm^{-2}, from Mischna & Shirley (2017), we obtained a damping time of 5.1 sols. A number of caveats are listed in Shirley et al. (2020); we nonetheless consider that a frictional damping time of O(10) sols is reasonable.

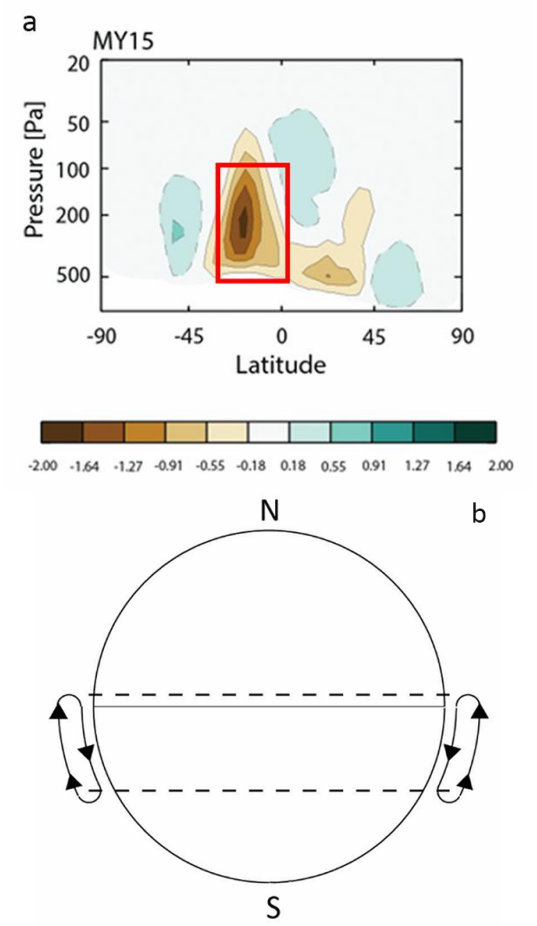

Fig. 3. (a) Zonal mean meridional stream function differences plot (forced – control) for the MY 15 simulation of Mischna & Shirley (2017). The scale gives units of 10^9 kg s^{-1}. Clockwise motions are represented in brown shades. The boxed area corresponds in latitude to the overturning cell sketched in (b). Topography was ignored for the calculations.

Characterizing the spin-down phase: The above scenario corresponds to periods when the forcing is greatly diminished, but in which momentum has previously been cumulatively added to the large-scale circulation. This corresponds to zero-crossings of the $d\boldsymbol{L}/dt$ waveform, and to extrema of the second derivative (Fig. 1). A rapid re-equilibration of the atmospheric wind and pressure fields may occur during such episodes. Atmospheric vorticity may be enhanced. Further, the extreme topographic relief of

the Martian surface may be expected to channel the resulting large-scale flows. Mars exhibits a number of preferred storm tracks. Flushing storms observed within the storm tracks frequently have durations of O(10) sols. Lastly, in addition, we recognize that the above frictional damping timescale corresponds reasonably well to the observed duration of the 2018 "triggering" regional storm (Shirley, Kleinböhl, et al., 2019), as illustrated here in Fig. 4.

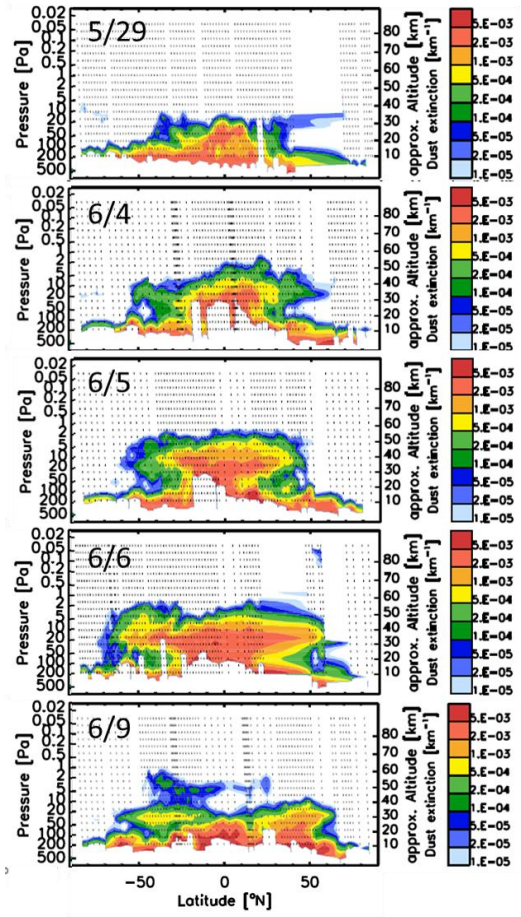

Fig. 4. MCS atmospheric dust extinction, within the Acidalia corridor, during the 2018 "triggering" regional storm (after Shirley, Kleinböhl, et al., 2019). Pre-storm conditions are shown on 29 May, while the decay phase of the regional storm is well advanced by 9 June. Dust layer peak altitudes increased from ~35 to ~60 km in this episode.

MCS observations confirm the existence of a strongly enhanced regional-scale Hadley circulation during the earliest days of the 2018 GDS (Shirley, Kleinböhl, et al., 2019; Fig. 4). Whether or not these observations may be explained by an atmospheric spin-down and re-equilibration process is an open question of considerable interest.

Challenges and opportunities: Will an early-season global-scale dust storm occur in 2025? Advance forecasts, addressing the likelihood of future GDS in MY 35-40, are provided in Shirley et al. (2020). The historic record (1877-present), together with solar system dynamical considerations, allows the identification of future "torque episodes." Objective rules for the identification of torque episodes are listed in Tables 6 and 9 of Shirley et al. (2020). Figure 5 illustrates torque episodes identified within the timespan of MY 38.

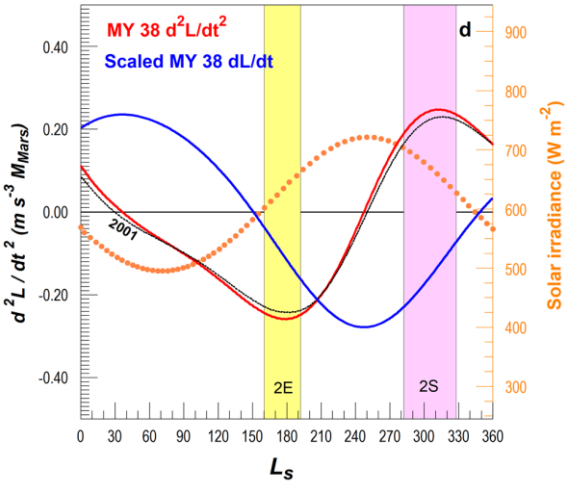

Fig. 5. Dynamical waveforms and identified torque episodes for Mars Year 38. The black dotted line illustrates the $d^2\mathbf{L}/dt^2$ waveform for MY 25, a GDS year (2001). The $d\mathbf{L}/dt$ waveform has been scaled by a factor of 10^{-8} for plotting. The yellow bar indicates an early-season torque episode, while purple identifies a post-solstice torque episode.

Figure 5 shows a close correspondence between the $d^2\mathbf{L}/dt^2$ waveforms for 2025-26 and 2001, an early-season GDS year (MY 25). The early-season torque episode of Fig. 5 begins on 24 October 2025 (L_s=160°). Shirley et al. (2020) conclude that this represents the highest likelihood interval for a future GDS between now and MY 40. MY 38 is likewise in-family with the three GDS years plotted in the lower panel of Fig. 1 (1909, 1977, 2001). All three of these GDS originated in Mars' southern hemisphere, in the vicinity of Hellas and/or Noachis. Priority should be given to observing campaigns that can comprehensively characterize atmospheric phenomena during this future torque episode.

We have already noted several deficiencies of past numerical modeling efforts. In addition, we note that the triggering mode illustrated in Fig. 1 had not yet been recognized, and that our temporal sampling interval (20° of L_s) was too coarse to resolve pulses of frictional damping in association with episodes of circulatory reorganization. The c value previously employed may in addition have been underestimated.

Atmospheric numerical models are unlikely to correctly represent atmospheric processes if some key physics is omitted. This applies to model studies employing data assimilation, as well as to investigations not constrained by concurrent observations.

Incorporation of orbit-spin coupling accelerations within state-of-the art MGCMs is strongly recommended.

Annotated Bibliography:

Prior Work	Principal Findings
P1: Shirley, J. H., Solar System Dynamics and Global-scale dust storms on Mars, *Icaru* s 251, 128, 2015	R1. **Discovery** of correlations linking historic Martian global dust storms (GDS) with variations in Mars orbital angular momentum with respect to inertial frames
	R2. First **published forecast** calling for a GDS in 2018
P2: Shirley, J. H., Orbit-spin Coupling and the Circulation of the Martian Atmosphere, *Planetary & Space Science* 141, 1-16, 2017	R3. **Derivation** of the **coupling equation** and demonstration of **quantitative sufficiency**
	R4. **Prediction**: Orbital variations drive cycles of intensification and relaxation of atmospheric circulations
P3: Shirley, J. H., and M. A. Mischna, Orbit-spin Coupling and the Interannual Variability of global-scale dust storm occurrence on Mars. *Planetary & Space Science* 139, 37-50, 2017	R5. First **formal statistical test** of the circulatory intensification-relaxation prediction of the orbit-spin coupling hypothesis
	R6. Second published forecast calling for a GDS in 2018
P4: Mischna, M. A., & J. H. Shirley, Numerical Modeling of Orbit-spin Coupling Accelerations in a Mars General Circulation Model: Implications for Global Dust Storm Activity, *Planetary & Space Science* 141, 45-72, 2017	R7. **Hypothesis testing** employing numerical simulations of an atmospheric circulation with orbit-spin coupling. **Confirmation** of the **prediction** of driven cycles of circulatory intensification within the modified GCM, claiming **proof of concept**
	R8. **Improved agreement with observations**: First-ever year-by-year **replication of observed planetary-scale atmospheric anomalies,** without the need to pre-condition state variables within the model
	R9. Third published forecast calling for a GDS in 2018
	R10. Identification of a **diagnostic observable**: Intermittent cycles of itensification and relaxation of **meridional overturning circulations**
P5: Newman, C. E., C. Lee, M. A. Mischna, M. I. Richardson, and J. H. Shirley, An initial assessment of the impact of postulated orbit-spin coupling on Mars dust storm variability in fully interacive dust simulation. *Icarus* 31, 649-668, 2019	R11. Second GCM investigation demonstrating **proof of concept**. The inclusion of orbit-spin coupling accelerations dramatically inproves the model's skill at predicting GDS and non-GDS years compared to a model without forcing
	R12. Fourth published forecast calling for a GDS in 2018
P6: Shirley, J. H., C. E. Newman, M. A. Mischna, & M. I. Richardson. Replication of the Historic Record of Martian Global Dust Storm Occurrence in an Atmospheric General Circulation Model, *Icarus* 317, 197-208, 2019	R13. **Improved agreement with observations**: The MarsWRF GCM, with orbit-spin coupling, **reproduces the historic record of Martian GDS** with a success rate of **77%**.
P7: Shirley, J. H., A. Kleinböhl, D. M. Kass, L. J. Steele, N. G. Heavens, S. Suzuki, S. Piqueux, J. T. Schofield, and D. J. McCleese, Rapid Expansion and Evolution of a Regional Dust Storm in the Acidalia Corridor During the Initial Growth Phase of the Martian Global Dust Storm of 2018, *Geophysical Research Letters* 46, e2019GL084317, 2019	R14. **Real-time observation of predicted effects**: The regional -scale "triggering storm" that initiated the 2018 global dust storm was powered-up by an intensified meridional overturning circulation. Spacecraft observations unambiguously record and resolve the **diagnostic observable** for orbit-spin coupling
P8: Shirley, J. H., R. J. McKim, J. M. Battalio, & D. M. Kass, Orbit-spin Coupling and the Triggering of the Martian Planet-encircling Dust Storm of 2018, *Journal of Geophysical Research-Planets* 125, e2019JE006077, 2020	R15. All historic Martian global dust storms are shown to be associated with dynamically and statistically defined **torque episodes**.
	R16. Sub-seasonal time resolution is achieved for hindcasting and for routine **forecasting of intervals of atmospheric instability** on Mars for the years 2020-2030